

# Development of the Timing System for the Bunch-to-Bucket Transfer between the FAIR Accelerators

Dissertation  
for attaining the doctoral degree  
of Natural Sciences

submitted to the Faculty of Physics  
of the Johann Wolfgang Goethe Universität  
in Frankfurt am Main, Germany

by  
Jiaoni Bai  
born in Taiyuan, Shanxi Province, China

Frankfurt am Main 2017  
(D 30)

accepted by the Faculty of Physics of the Johann Wolfgang Goethe University  
as a dissertation.

Dekan:	Prof. Dr. Owe Philipsen
Gutachter:	Prof. Dr. Oliver Kester
	Prof. Dr. Ulrich Ratzinger
Date of disputation:	07. May. 2017

I would like to dedicate this dissertation to my dear parents,  
loving husband and good friends ...

# Acknowledgement

First and foremost, I would like to thank my professor Prof. Dr. Oliver Kester. It is a great honour for me to be his Ph.D. student. He gave me the chance to study at Goethe Universität, Frankfurt am Main and work in GSI for this interesting Ph.D. topic. I appreciate all his contributions of time and ideas to make my Ph.D. successful. I was deeply influenced by his enthusiasm for his research and his selfless support for his students. I was thankful for his support, that I participated many international conferences, schools and workshops. This experience enriched my life and broadened my horizons.

I wish to express my sincere gratitude to Dr. David Ondreka and Dr. Dietrich Beck for their supervision, valuable guidance and helpful suggestions throughout my Ph.D. study. I have been greatly lucky to have so good supervisors, who cared much about my work and who answered my doubts patiently. They were like a lighthouse in the ocean, which guides me in the right direction. They are not only my scientific supervisors, but also my mentors. They encouraged and motivated me during tough time of my Ph.D. Hence, I will keep a positive attitude and keep moving forward when I face with challenges, difficulties and temporary setbacks in the future.

I would like to acknowledge all colleagues in the timing group, CSCO department, GSI, Mathias Kreider, Stefan Rauch, Marcus Zweig, Alexander Hahn and former employee Dr. Wesley Terpstra, who provided me much technical support. I would like to extend my appreciation to department leader Dr. Ralph Bär, who gave much support for my Ph.D. topic. Thanks for their friendship and collaboration. I am especially grateful for the group member Cesar Prados, by whom I learned not only technical knowledge, but also how to work efficiently and how to become a good engineer. I would also like to thank Matthias Thieme, who provided me the devices for the test setup and Marko Stanislav Mandakovic for the discussion about the MPS. I would like to extend gratitude to Dr. Udo Krause and Peter Kainberger for the information about the GSI control system.

I am also thankful for the good cooperation with Thibault Ferrand, who studies at Technische Universität Darmstadt and works in PBRF department, GSI. Thanks for his valuable contribution of the development of the LLRF system for the B2B transfer system for FAIR. I would like to extend my sincerest thanks and appreciation to PBRF department leader Prof. Dr. Ing. Harald Klingbeil for his support. In addition, a special thanks is also extended to Dr. Dieter Lens and Stefan Schäfer for their technical support. Thanks for Dr. Bernhard Zipfel to give me support about BuTiS.

I wish to express my sincere gratitude to SBES department leader Dr. Markus Steck for his technical support of ESR and CRYRING, Dr. Udo Blell in PBHV department for the technical support of kicker and Dr. Michael Block in SHE-P department for the supply of two SRS function generators.

I must express my gratitude to GSI and also HGS-HiRe, who provided the scholarship which allowed me to undertake this research.

Lastly, I would like to thank my family for all their love and encouragement. My parents always support me to pursuing my dreams. Most of all, my loving husband Zigao Li is so appreciated, who always encourages me to realize my dreams. Thank you.

Jiaoni Bai  
Darmstadt, September 2016

# Abstract

The Facility for Antiproton and Ion Research (FAIR) is a new international particle accelerator facility under construction at GSI Helmholtz center for Heavy Ion Research GmbH. It is aiming at providing high-energy beams of ions from hydrogen to uranium with high intensities, as well as beams of rare isotopes and beams of antiprotons. The FAIR accelerators will be supplied with ion beams by the GSI accelerator facilities, which comprises the injectors for the FAIR accelerators. The injection chain consists of the linear accelerator UNILAC and the heavy ion synchrotron SIS18. In addition, the GSI accelerator facility comprises the experimental storage ring (ESR) and the CRYRING, which complement the planned accelerators of FAIR. The FAIR accelerator complex in its full version consists of many ring accelerators with different functionality. The FAIR facility in its start version will consist of three circular accelerators, which add to the three rings at GSI. The driver accelerator of FAIR is the fast ramping, superconducting heavy ion synchrotron SIS100, that allows the acceleration of the most intense beams of stable elements. The primary beams are used to produce secondary particles, which are delivered to the cooler ring (CR) via high energy separators. The CR will accumulate the secondary beams and improve their quality by stochastic cooling. The storage rings HESR will host a large fraction of the experiment platforms with a variety of different experiments. These circular accelerators of GSI and FAIR have different ratios in their circumference. For example, the circumference ratio between the SIS100 and the SIS18 is an integer and between the SIS18 and the ESR is close to an integer and between the CR and the HESR is far away from an integer. The ring accelerators are connected via a complicated system of beam transfer lines, targets for the secondary particle production and the high energy separators mentioned above. For FAIR, not only the primary beams are required to be transferred from one ring to another, but also the secondary beams. e.g. the antiproton or rare isotope beams produced by the pbar target, the Fragment Separator (FRS) or the Super FRS. An important topic for this system of accelerators is the precise transfer of beam between the different machines. Bunches of one ring must be transferred into buckets of another ring within an upper bound time constraint (e.g. 10 ms for most FAIR use cases) and with an acceptable bunch-to-bucket injection center mismatch (e.g.  $\pm 1^\circ$  for most FAIR use cases). Hence, a flexible FAIR Bunch-to-Bucket (B2B) transfer system is required to realize the different complex bunch-to-bucket transfers between the FAIR rings in the future. In the focus of the system development is the transfer from the SIS18 to the SIS100, which will be tested at GSI on the transfer from the SIS18 to the ESR and from the ESR to the CRYRING. The system is based on the existing technical basis at GSI, the low level radio frequency (LLRF) system and the FAIR control system. It coordinates with the Machine Protection System, which protects SIS100 and subsequent accelerators and experiments from damage caused

by high intensity primary beams in case of malfunctioning. Besides, it indicates the beam status and the actual beam injection time for the beam instrumentation and diagnostics.

In this thesis the basic idea, the basic procedure and the conceptual realization of the bunch-to-bucket transfer system are described in detail and the mathematical evaluation of the required timing parameters is presented. In order to trigger the extraction and injection kickers correctly, the FAIR B2B transfer system is composed of two synchronization processes, a coarse synchronization and a fine synchronization. The coarse synchronization gives a coarse time frame, within which bunches are transferred into buckets with a bunch-to-bucket center mismatch smaller than a well defined bound. This time frame is called the “synchronization window“. With the synchronization window, the extraction and injection kickers are triggered at the correct time in order to transfer bunches into correct empty buckets. The process of the kicker trigger at the correct time is the “fine synchronization“. The fine synchronization is achieved based on a bucket indication signal plus a fixed delay. The bucket indication signal is derived from the rf revolution frequency signal and always indicates the first bucket. A fixed delay is used to indicate the correct buckets to be filled.

The coarse synchronization is based on the phase difference between the two rf systems of two rings, which is obtained by the phase deviation measurement between the rf system and a campus-wide distributed synchronization reference signal at both rings. When the circumference ratio between two rings is an integer, the phase difference between the two rf systems is constant. In order to get the correct phase difference, the phase of either (or both) rf systems must be shifted by means of an rf frequency modulation. This is called “phase shift method“. After the rf frequency modulation, the phase difference between the two rf systems is correct and the synchronization window is infinitely long theoretically. When the circumference ratio between two rings is not an integer, the phase difference between the two rf systems varies periodically. The synchronization window brings a symmetric time frame with respect to the time, when the phase difference between two rf systems is closest to the required phase difference. This is called “frequency beating method“. The frequency beating method is also applicable when the circumference ratio between two rings is an integer. In this case, the rf frequency of either (or both) rf systems is detuned at the end of the acceleration ramp, so that two rf systems are beating. For the FAIR project, the frequency beating method is preferable, because it is applicable for all beam transfer scenarios. In addition, it reduces the synchronization time, because the rf frequency detune is executed during the rf acceleration ramp. For the phase shift method, the rf frequency modulation must be executed slowly enough at the rf flattop for the beam to follow, which uses much longer time. However, there are also some advantages of the phase shift method. The synchronization window is relatively long and the bunch-to-bucket injection center mismatch is approximately  $0^\circ$ . Besides, the duration of the rf frequency modulation is known in advance and the time point for the transfer is predictable. The phase of the rf system can jump to a desired value, when there is no bunch at the ring.

In this thesis, a systematic investigation is done from the beam dynamics, timing requirement of the transfer and kicker trigger perspectives. The timing perspective includes the accuracy of the start of the synchronization window, the characterization of the White Rabbit network for the B2B transfer, the flow chart and the time

constraints of the system. A test setup of the timing system required for the transfer using the frequency beating method is presented, which proves that the firmware running on the soft CPU meets the functional requirement and the time constraints. Finally, all FAIR use cases with the frequency beating method are discussed.

The dissertation plays a significant important role for the realization of the FAIR B2B transfer system of the released version and the further practical application of the system to all FAIR use cases.



# Kurzfassung

Die *Facility for Antiproton and Ion Research* (FAIR) ist eine im Bau befindliche, internationale Teilchenbeschleunigeranlage, die unter der Leitung von der GSI Helmholtzzentrum für Schwerionenforschung GmbH errichtet wird. Sie hat zum Ziel, hochenergetische Ionenstrahlen zu erzeugen. FAIR wird in der Lage sein Strahlen höchster Intensität für Elemente von Wasserstoff bis Uran zur Verfügung zu stellen und darüber hinaus in der Lage sein Antiprotonen und exotische Nuklide zu erzeugen. Die existierende Beschleunigeranlage der GSI wird der Injektor der FAIR-Beschleuniger sein und umfasst den Linearbeschleuniger UNILAC und das Schwerionen-Synchrotron SIS18. Desweiteren umfasst die GSI Beschleunigeranlage zwei Speicherringe, den Experimentierspeicherring (ESR) und den CRYRING. Der FAIR-Beschleunigerkomplex in seiner Startversion, besteht aus vielen Ringbeschleunigern mit unterschiedlichen Funktionalitäten und Aufgaben. Der Primärstrahltrieb ist das supraleitende Schwerionen-Synchrotron SIS100. Für die Präparation der Sekundärstrahlen und die Experimente dienen der *Collector Ring* (CR) und der *High Energy Storage Ring* (HESR). Die Ringbeschleuniger der GSI und von FAIR haben sehr unterschiedliche Verhältnisse ihrer Umfänge. Zum Beispiel ist das Umfangsverhältnis zwischen dem SIS18 und dem SIS100 ganzzahlig, zwischen dem SIS18 und dem ESR annähernd ganzzahlig und zwischen dem CR und dem HESR ist es weit weg von einem ganzzahligen Verhältnis. Alle FAIR-Ringbeschleuniger sind über Strahltransportlinien, die Targets zur Produktion von Sekundärteilchen und den zugehörigen Hochenergieseparatoren verbunden. Für FAIR ist es nicht nur erforderlich Primärstrahlen von einem zum anderen Ring zu transferieren, sondern auch Sekundärstrahlen, wie Antiprotonen oder exotische Nuklide die im Antiprotonen-Target, im Fragmentseparator oder im Suprafragmentseparator erzeugt werden, wieder in Speicherringe einzufangen. Zudem müssen *bunch* von einem Ring in *bucket* eines anderen Rings, innerhalb einer bestimmten Zeit (z.B. unter 10 ms in fast allen FAIR-Anwendungsfällen) und mit einem akzeptablen *Bunch-to-Bucket*-Injektions-Mittenversatz (z.B. unter  $\pm 1^\circ$  in den meisten FAIR-Anwendungsfällen) transferiert werden. Daher ist ein flexibles *FAIR Bunch-to-Bucket (B2B) transfer system* erforderlich, um die verschiedenen und komplexen B2B-Transfers zwischen den zukünftigen FAIR-Ringen realisieren zu können. Im Fokus dieser Arbeit ist natürlich der Teilchentransfer vom SIS18 zum SIS100, welcher am Beispiel des Transfers zwischen SIS18 zum ESR und vom ESR zum CRYRING an der GSI getestet werden kann. Das System wird auf Basis der für FAIR vorgesehen, technischen Infrastruktur entwickelt. Dazu zählen das *FAIR low level radio frequency (LLRF) system* und das Kontrollsystem für FAIR. Das *FAIR B2B transfer system* hat eine Schnittstelle zum FAIR-Maschinenschutzsystem (*machine protection system*), welchen das SIS100 und die nachgeschalteten Beschleuniger und Experimente vor Schaden bedingt durch Strahlverlusten bewahrt. Außerdem wird der Status des Strahls und

der Zeitpunkt der Strahlinjektion vom *FAIR B2B transfer system* an die Geräte der Strahldiagnose gemeldet.

Diese Doktorarbeit stellt vor allem die Grundidee, das grundlegende Verfahren und die konzeptionelle Realisierung des *FAIR B2B transfer system* vor. Darüber hinaus werden die Anforderungen an das Timing analytisch ermittelt und vorgestellt. Das *FAIR B2B transfer system* nutzt einen zweistufigen Synchronisationsprozess, um den exakten Kickzeitpunkt zu bestimmen. In der ersten Stufe, der „Grosyn-chronisation“ gibt ein Synchronisationsfenster ein Zeitintervall vor, indem der B2B-Injektions-Mittenversatz zwischen *bunch* und *bucket* innerhalb der geforderten Toleranzgrenze bleibt. Innerhalb dieses Synchronisationsfensters müssen die Kicker zum richtigen Zeitpunkt gezündet werden, um die *bunch* in die richtigen, leeren *bucket* der Zielmaschine zu schießen. Das übernimmt die sogenannte „Feinsynchronisation“. Die „Feinsynchronisation“ ist das *bucket indication signal*, welches über ein festes Delay verzögert wird. Das *bucket indication signal* wird von den Hochfrequenzsignalen (HF-Signal) der Umlauffrequenzen abgeleitet und kennzeichnet immer das erste *bucket*. Ein weiteres Delay wird dazu benutzt, um die folgenden, zu befüllenden *bucket* zu kennzeichnen.

Für die Grosynchronisation wird die Phasendifferenz zwischen den HF-Signalen der Quell- und Zielmaschine gemessen. Die Phasendifferenz erhält man, indem man die Phasenabweichung der HF-Signalen beider Ringe gegen ein campusweit verteiltes *synchronization reference signal* vermisst. Wenn das Umfangsverhältnis beider Ringe ganzzahlig ist, bleibt die Phasendifferenz der beiden HF-Signale während des Transfers konstant. Um die richtige Phasendifferenz zu erreichen, muss die Phase eines (oder beider) HF-Systeme mithilfe einer Frequenzmodulation verschoben werden. Das nennen wir die *phase shift method*. Nach der exakten Ausrichtung der Phasen, bleibt die gewünschte Phasendifferenz konstant und ermöglicht, theoretisch ein unendlich langes Synchronisationsfenster. Wenn das Umfangsverhältnis beider Ringe nicht ganzzahlig ist, verändert sich die Phasendifferenz periodisch. Innerhalb einer Periode gibt es dann nur einen Zeitpunkt, zu dem die Zielphase erreicht wird. Davor und danach kommt es zu einem B2B-Injektions-Mittenversatz zwischen *bunch* und *bucket*. Das nennen wir die *frequency beating method*. Diese ist auch anwendbar, wenn das Umfangsverhältnis beider Ringe ganzzahlig ist. In diesem Fall wird die HF-Frequenz eines (oder beider) HF-Systeme am Ende der Beschleunigungsrampe leicht verstimmt, sodass sich eine Schwebungsfrequenz zwischen den HF-Systemen der Quell- und Zielmaschine ergibt. Für FAIR wird die *frequency beating method* präferiert, weil diese Methode für sämtliche Transferszenarien bei FAIR anwendbar ist. Außerdem kann mit dieser Methode Zeit gespart werden, weil die Frequenzverstimmung während der Beschleunigungsrampe durchgeführt wird. Zur Erinnerung: Bei der *phase shift method* muss die Frequenzmodulation auf *rf flattop* langsam genug ausgeführt werden, damit der Strahl stabil bleibt. Das kostet viel Zeit. Dennoch gibt es auch Vorteile, die für die *phase shift method* sprechen. Das Synchronisationsfenster ist theoretisch unendlich lang und der B2B-Injektions-Mittenversatz ist nahezu „Null“. Außerdem ist die Dauer der Frequenzmodulation vorab bekannt und der Transfer-Zeitpunkt ist exakt bestimmbar. Vorteilhaft ist auch, dass die gewünschte Phase des HF-Systems sprunghaft eingestellt werden kann, wenn sich kein *bunch* im Ring befindet.

Im Rahmen dieser Doktorarbeit wird eine systematische Untersuchung der strahldynamischen Aspekte, der zeitlichen Anforderungen an den B2B-Transfer-Prozess und

der Trigger-Szenarien für die Kicker-Auslösung durchgeführt. Die Timing-Betrachtungen berücksichtigen die erforderliche Genauigkeit für den Beginn des Synchronisationsfensters, die Charakterisierung des *White Rabbit* Netzwerks, das Flussdiagramm mit Timing-Bedingungen für das *FAIR B2B transfer system*. Danach wird ein Messaufbau zur Bestimmung des Timings vorgestellt, der dazu verwendet wird die *firmware*, die auf einer *soft-CPU* ausgeführt wird, hinsichtlich der Einhaltung der Timing- und Funktionsanforderungen zu überprüfen. Zum Schluss werden alle FAIR-Anwendungsfälle, bei denen die *frequency beating method* verwendet wird, erörtert.

Diese Doktorarbeit spielt eine wichtige Rolle bei der Realisierung der veröffentlichten Version des *FAIR B2B transfer system* und der weiteren praktischen Anwendung des Systems für alle FAIR-Transferszenarien.

# Contents

<b>Abstract</b>	<b>i</b>
<b>1 Introduction</b>	<b>1</b>
1.1 Bunch-to-Bucket Transfer worldwide . . . . .	4
1.2 Objectives, Contribution and Structure of the Dissertation . . . . .	5
<b>2 Theoretical Background</b>	<b>8</b>
2.1 Bunch and Bucket . . . . .	8
2.2 Phase Difference . . . . .	14
2.2.1 Circumference Ratio is an Integral . . . . .	16
2.2.2 Circumference Ratio is close to an Integer . . . . .	17
2.2.3 Circumference Ratio is far away from an Integer . . . . .	18
2.3 Phase Match of Two Rf Systems . . . . .	20
2.3.1 Phase Shift Method . . . . .	21
2.3.2 Frequency Beating Method . . . . .	24
2.4 Synchronization of Extraction and Injection Kicker Magnets . . . . .	26
<b>3 Technical Basis for the FAIR B2B Transfer System</b>	<b>30</b>
3.1 FAIR Control System . . . . .	30
3.1.1 Bunch Phase Timing System . . . . .	30
3.1.2 General Machine Timing System . . . . .	31
3.1.3 Settings Management . . . . .	32
3.1.4 FESA . . . . .	32
3.2 Low-Level RF System . . . . .	32
3.2.1 Local Cavity Synchronization . . . . .	33
3.2.2 Longitudinal Feedback System . . . . .	34
3.3 Machine Protection System . . . . .	35
<b>4 Concept of the FAIR B2B Transfer System</b>	<b>36</b>
4.1 Basic Idea . . . . .	36
4.1.1 Phase Alignment . . . . .	36
4.1.2 Trigger of Extraction and Injection Kickers . . . . .	38
4.1.2.1 Bucket Indication Signal . . . . .	39
4.1.2.2 Extraction and Injection Kicker Delay Compensation	40
4.2 Basic Procedure . . . . .	41
4.3 Realization . . . . .	42
4.3.1 Phase Measurement and Corresponding Timestamp of Each Rf System . . . . .	45

4.3.1.1	Measurement of Actual Phase Values of Each Rf System . . . . .	45
4.3.1.2	Phase Extrapolation of Each Rf System . . . . .	46
4.3.1.3	Timestamp of the Extrapolated Phase . . . . .	47
4.3.2	Exchange of Measured Data . . . . .	48
4.3.3	Rf Synchronization . . . . .	49
4.3.3.1	Rf Synchronization with the Phase Shift Method . . . . .	50
4.3.3.2	Rf Synchronization with the Frequency Beating Method . . . . .	50
4.3.4	Coarse Synchronization . . . . .	51
4.3.5	Bucket Label . . . . .	53
4.3.6	Bucket Label for the Normal Extraction and Injection . . . . .	54
4.3.7	Maximum Bunch Spacing Label for the Emergency Extraction . . . . .	54
4.3.8	Fine Synchronization of Extraction and Injection Kickers . . . . .	56
4.3.9	B2B Transfer Status Check . . . . .	57
4.4	Data Flow . . . . .	57
4.5	Comparison between the FAIR B2B Transfer System and Current B2B Transfer . . . . .	61

## 5 Realization and Systematic Investigation of the FAIR B2B Transfer System 63

5.1	Beam Dynamic Analysis of two Synchronization Methods for the B2B Transfer from SIS18 to SIS100 . . . . .	63
5.1.1	Beam Dynamics of the Phase Shift Method for $U^{28+}$ . . . . .	64
5.1.1.1	Longitudinal Dynamic Analysis . . . . .	68
5.1.1.2	Transverse Dynamics Analysis . . . . .	73
5.1.2	Beam Dynamics of the Frequency Beating Method for $U^{28+}$ . . . . .	73
5.1.2.1	Longitudinal Dynamics Analysis . . . . .	73
5.1.3	Beam Dynamics of the Phase Shift Method for $H^+$ . . . . .	73
5.1.3.1	Longitudinal Dynamics Analysis . . . . .	74
5.1.3.2	Transverse Dynamics Analysis . . . . .	74
5.1.4	Beam Dynamics of the Frequency Beating Method for $H^+$ . . . . .	75
5.1.4.1	Longitudinal Dynamics Analysis . . . . .	75
5.2	GMT Systematic Investigation . . . . .	75
5.2.1	Calculation of the Start of the Synchronization Window . . . . .	75
5.2.1.1	Uncertainty of the Phase Alignment . . . . .	76
5.2.1.2	Uncertainty of the Start of the Synchronization Window . . . . .	80
5.2.1.3	Requirement of the Accuracy of the Start of the Synchronization Window . . . . .	81
5.2.2	Characterization of the WR Network for the B2B Transfer . . . . .	82
5.2.2.1	Traffic on the WR Network . . . . .	83
5.2.2.2	Frame Loss of the WR Network for the B2B Transfer . . . . .	84
5.2.2.3	WR Network Test Setup . . . . .	85
5.2.2.4	Measurements . . . . .	88
5.2.2.5	Measurements Result . . . . .	90
5.2.2.6	Result Discussion . . . . .	90
5.2.2.7	Conclusion of the Network Measurements . . . . .	91
5.2.3	Flowchart of the system for SCUs . . . . .	92

5.2.4	Time Constraints . . . . .	96
5.3	Kicker Systematic Investigation . . . . .	98
5.3.1	Simultaneous Trigger for Extraction Kicker Magnets in a Com- mon SIS18 Tank . . . . .	98
5.3.2	A Fixed Trigger Delay between Extraction Kicker Magnets in the SIS18 1 <sup>st</sup> and 2 <sup>nd</sup> Tanks . . . . .	100
5.3.3	Simultaneous Trigger for SIS100 Injection Kicker Magnets . .	102
5.4	A Test Setup for Timing Aspects . . . . .	104
5.4.1	Test Setup . . . . .	104
5.4.2	Comparison between the Test Setup and the Final Setup . . .	106
5.4.3	Procedure . . . . .	106
5.4.4	Functional Test Result . . . . .	109
5.4.5	Measurement Result Discussion . . . . .	110
<b>6</b>	<b>Application of the FAIR B2B Transfer System to FAIR Accelera- tors</b>	<b>112</b>
6.1	Circumference Ratio is an Integer . . . . .	113
6.1.1	$U^{28+}$ B2B Transfer from SIS18 to SIS100 . . . . .	115
6.1.2	$H^+$ B2B Transfer from SIS18 to SIS100 . . . . .	115
6.2	Circumference Ratio is close to an Integer . . . . .	117
6.2.1	$h=4$ B2B Transfer from SIS18 to ESR . . . . .	117
6.2.2	$h=1$ B2B Transfer from SIS18 to ESR . . . . .	119
6.2.3	B2B transfer from ESR to CRYRING . . . . .	119
6.3	Circumference Ratio is far away from an Integer . . . . .	121
6.3.1	$H^+$ B2B Transfer from SIS100 to CR . . . . .	122
6.3.2	RIB B2B Transfer from SIS100 to CR . . . . .	123
6.3.3	B2B Transfer from CR to HESR . . . . .	123
6.3.4	RIB B2B Transfer from SIS18 to ESR via the FRS . . . . .	124
6.4	Summary . . . . .	126
	<b>Conclusion and Outlook</b>	<b>130</b>
	<b>Zusammenfassung</b>	<b>134</b>
	<b>Glossary</b>	<b>139</b>
	<b>Abbreviations</b>	<b>143</b>
	<b>Symbols</b>	<b>147</b>
<b>A</b>	<b>FAIR B2B Transfer Related Timing Frames</b>	<b>153</b>
<b>B</b>	<b>Timing Frames Transfer for the FAIR B2B Transfer System</b>	<b>155</b>
<b>C</b>	<b>Parameters of FAIR B2B Transfer Use Cases</b>	<b>157</b>
C.1	Parameters of the B2B Transfer from SIS18 to SIS100 . . . . .	157
C.2	Parameters of the B2B Transfer from SIS18 to ESR . . . . .	158
C.3	Parameters of the B2B Transfer from SIS18 to ESR via the FRS . . .	159
C.4	Parameters of the B2B Transfer from ESR to CRYRING . . . . .	160
C.5	Parameters of the B2B Transfer from CR to HESR . . . . .	161

## CONTENTS

---

C.6 Parameters of the B2B Transfer from SIS100 to CR . . . . .	162
<b>D Parameters of the FAIR B2B Transfer System from Settings Management</b>	<b>163</b>
<b>E Parameters of FAIR Kicker Magnets</b>	<b>165</b>
<b>F Configuration for the Test Setup</b>	<b>166</b>
F.1 Configuration of the B2B source SCU . . . . .	166
F.2 Configuration of the B2B target SCU . . . . .	166
F.3 Configuration of the Trigger SCU . . . . .	167
F.4 Configuration of the packETH . . . . .	167
<b>Bibliography</b>	<b>167</b>
<b>List of Figures</b>	<b>167</b>
<b>List of Tables</b>	<b>170</b>
<b>Publications</b>	<b>173</b>

# Conclusion and Outlook

The FAIR project is aiming at providing high-energy beams of ions from hydrogen to uranium, antiproton and rare isotope with high intensities. The existing accelerator facility of GSI and the future FAIR facility employ a variety of circular accelerators like heavy ion synchrotrons (the SIS18 and the SIS100) and storage rings (the ESR, the CRYRING, the CR and the HESR) for beam preparation and experiments. Bunches are required to be transferred into rf buckets among GSI and FAIR ring accelerators for different purposes. Without the proper transfer, the beam will be subject to various beam quality (emittance) deterioration and even to beam losses. Hence, the proper bunch-to-bucket transfer between two rings is of great importance for FAIR and is the topic, which has been investigated in this thesis. Although an implementation of the B2B transfer from the SIS18 to the ESR exists, this solution is not applicable for the new FAIR accelerator complex. Because it is realized based on the GSI control system, an event based system, which will be replaced by the FAIR control system in future. The FAIR control system is based on the sub-nanosecond synchronization White Rabbit network. Besides, it doesn't support the B2B transfer with the phase shift method and with the complex bucket pattern. It is not capable to transfer beams via targets. Hence, a new FAIR B2B transfer system is required, which relies on the FAIR technical basis, the FAIR control system and the low level rf system.

The conceptual realization of the FAIR B2B transfer system was introduced in this thesis for the first time. It achieves the most FAIR B2B transfers with a tolerable bunch-to-bucket injection center mismatch (e.g.  $\pm 1^\circ$ ) and within an upper bound time (e.g. 10 ms). It supports both the phase shift and frequency beating methods. It is flexible to support the beam transfer between two rings with different ratios in their circumference and several B2B transfers running at the same time, e.g. the B2B transfer from the SIS18 to the SIS100 and at the same time the B2B transfer from the ESR to the CRYRING. It is capable to transfer beam of different ion species from one machine cycle to another. It has the ability to transfer the beam between two rings via the FRS, the pbar target and the Super FRS. It allows various complex bucket filling pattern. In addition, it coordinates with the MPS system, which protects the SIS100 and subsequent accelerators or experiments from beam induced damage.

A number of criteria for the preservation of beam qualities during the rf frequency modulation of the phase shift method were presented in the next place in this thesis. Additionally the beam reaction accompanying with three rf frequency modulation examples were analyzed for the SIS18 beams. According to the beam dynamic analysis, there is a maximum value for the rf frequency modulation, which comes from the constraint of the momentum shift. The first derivative of the rf frequency modulation must be continuous and small enough to guarantee the size



of the running bucket. The second derivative must be small enough to guarantee the change of the synchronous phase slow enough for the beam to follow, which is reflected by the parameter of the adiabaticity. In order to guarantee the bucket area factor larger than 80% and the adiabaticity smaller than  $10^{-4}$ , for the SIS18 200 MeV/u  $U^{28+}$  beam,  $|\Delta f_{rf}|$  must be smaller than 8.137 kHz and  $|\frac{d\Delta f_{rf}}{dt}|$  must be continuous and smaller than 95 Hz/ms and  $|\frac{d^2\Delta f_{rf}}{dt^2}|$  must be smaller than 70 Hz/ms<sup>2</sup>. For the SIS18 4 GeV  $H^+$  beam,  $|\Delta f_{rf}|$  must be smaller than 283 Hz and  $|\frac{d\Delta f_{rf}}{dt}|$  must be continuous and smaller than 1.9 Hz/ms and  $|\frac{d^2\Delta f_{rf}}{dt^2}|$  must be smaller than 0.2 Hz/ms<sup>2</sup>. In regard with these requirements, the sinusoidal and parabolic rf frequency modulation profiles with a certain duration were checked for the SIS18  $U^{28+}$  beam. Both two modulation profiles meet the requirements and keep the beam stable. However, compared with the parabolic modulation, the sinusoidal modulation has the smaller adiabaticity. Hence, the sinusoidal modulation is preferable for the phase shift method. The sinusoidal rf frequency modulation for the SIS18  $U^{28+}$  needs 7 ms and the sinusoidal rf frequency modulation for the SIS18  $H^+$  needs approximately 50 ms for the phase shift of  $\pi$ .

In addition to the analysis from the viewpoint of beam dynamics, two test setups were built. The first test setup was used to characterize the WR network for the B2B transfer. According to the test result, the tolerable number of WR switch layers for the B2B transfer depends not only on the upper bound transfer latency (e.g. 400 ms), but also the tolerable frame error rate of the B2B transfer system. If no forward error correction mechanism is used for the B2B transfer, the number of WR switch layers is mainly decided by the tolerable frame error rate. If for instance one lost frame is tolerable every two month, the maximum 38 WR switches can be used between the B2B related SCUs and DM and the maximum 8 WR switches can be used between the B2B related SCUs. If specific forward error correction mechanisms are used, the number of WR switch layers depends mainly on the tolerable transfer latency. In this case, the tolerable number of WR switches is 67 between the B2B related SCUs and DM and the tolerable number of WR switches is 13 between the B2B related SCUs. In the second test setup, **the firmware of the FAIR B2B transfer system was evaluated, which was running on the soft CPU, LatticeMico32, of the SCUs.** The running time of tasks of the firmware was measured. It has proven that the firmware running on the LatticeMico32 of the SCUs meets the requirement of the timing constraints, when the related System-on-Chip bus is not occupied by any other applications at the same time as the firmware is running.

Furthermore, the propagation of the measurement uncertainties (e.g. **the 0.1° phase measurement uncertainty, the 100 ps BuTiS clock uncertainty and the 1 ns timestamp measurement uncertainty**) to the time of the phase alignment was checked for all FAIR use cases in this thesis. The bunch-to-bucket injection center mismatch is deteriorated by the time uncertainty of the phase alignment in various degrees. For some use cases the bunch-to-bucket injection center mismatch is seriously deteriorated. e.g. the mismatch is deteriorated by 37% for the  $U^{28+}$  B2B transfer from the SIS18 to the SIS100. However, the deteriorated mismatch still meet the requirement smaller than  $\pm 1^\circ$ . Hence, the measurement uncertainties are acceptable for the FAIR B2B transfer system. In addition, the requirement of the accuracy of the start of the synchronization window for all FAIR use cases was also checked in this thesis, the most stringent requirement of the accuracy comes from

the  $h=1$  B2B transfer from the SIS18 to the ESR, which is approximately 500 ns.

Besides, the different trigger scenarios of the SIS18 extraction and SIS100 injection kicker magnets were investigated. The nine SIS18 extraction kicker magnets are distributed into two tanks. The kicker magnets in each tank can be triggered simultaneously when the bunch gap is at least 25% of the cavity rf period. The four kicker magnets in the 2<sup>nd</sup> tank can be triggered a fixed delay after the trigger of the five kicker magnets in the 1<sup>st</sup> tank for all ion beams, when the bunch gap is at least 25% of the cavity rf period. The six SIS100 injection kicker magnets are evenly distributed in one tank. They can be fired instantaneously for all ion beams, when the bunch gap is at least 35% of the cavity rf period.

Finally, the application of the FAIR B2B transfer system with the frequency beating method for all FAIR use cases was demonstrated. It has been shown that for all primary beam transfers of FAIR use cases, the B2B transfer with the bunch-to-bucket injection center mismatch less than  $\pm 1^\circ$  and within the required B2B transfer time 10 ms can be achieved, because the circumference ratio between two rings is an integer or close to an integer. **However, the system is also required for the FAIR use cases that the secondary beams are generated by the pbar target, the FRS or the Super FRS with an arbitrary energy ratio between the primary and secondary beams.** For the rare isotope beam transfer from the SIS100 to the CR via the Super FRS with the 1.5 GeV/u primary beam energy and the 740 MeV/u secondary beam energy, the bunch-to-bucket injection center mismatch is only  $\pm 2.1^\circ$  by coincidence. For the antiproton B2B transfer from the SIS100 to the CR via the pbar target and the rare isotope beam transfer from the SIS18 to the ESR via the FRS, the bunch-to-bucket injection center mismatch is as large as  $\pm 40^\circ$ , which is far beyond the upper bound injection center mismatch.

The dissertation at hand comprises the important investigations for the FAIR B2B transfer system from the beam dynamics, timing and kicker trigger perspectives. However, there are still some investigations which are required for the final system operation:

- The synchronization between the magnetic horn after the pbar target and the antiproton beam to the  $\mu$ s order of magnitude.
- The synchronization between the bunch compressor of the SIS100 and the beam extraction.
- For several FAIR use cases of the secondary beam, the bunch-to-bucket injection center mismatch is larger than  $\pm 40^\circ$ . For these FAIR use cases, it is necessary to check whether the FAIR B2B transfer system can work together with specific beam accumulation methods, e.g. the barrier bucket or the unstable fixed point accumulation.

The FAIR B2B transfer system presented in the dissertation is applicable for all FAIR use cases. However, there is still potential for improvement. For the phase shift method, the rf frequency modulation must be slow enough (e.g. the 7 ms/50 ms sinusoidal modulation for the SIS18  $U^{28+}/H^+$  beam). In order to transfer bunches into buckets as soon as possible, the phase shift can be started during the acceleration ramp. At a certain time point during the acceleration, the phase difference between the two rf systems of the source and target rings is obtained with the help of the synchronization reference signal. There is a look-up table, which gives the phase

difference at the rf flattop according to the phase difference obtained at the certain time point. Then, an rf frequency modulation is superposed on the initial frequency pattern. With this new frequency pattern, the phase difference will be the required phase difference when the cavity rf frequency of the source and target rings reach the flattop.

# Zusammenfassung

FAIR hat zum Ziel, hochenergetische Ionenstrahlung für die Elemente Wasserstoff bis Uran, Antiprotonen und exotische Nuklide, mit höchsten Intensitäten zu erzeugen. Die existierende Beschleunigeranlage der GSI wie auch die zukünftige FAIR-Anlage nutzt eine unterschiedliche Ringbeschleuniger wie beispielsweise Schwerionensynchrotrons (das SIS18 und das SIS100) und auch Speicherringe (den ESR, den CRYRING, den CR und den HESR) zur **Präparation der Sekundärstrahlen für die Experimente**. Ein stabiler Transfer von *Bunchen* in *Buckets* zwischen allen GSI und FAIR-Ringbeschleunigern, ist aus verschiedenen Gründen erforderlich. Bei einem nicht ordnungsgemäßen Strahl-Transfer besteht die Gefahr, dass es zu einer Degeneration der Strahlqualität (z.B. einer Emittanzerhöhung), bis hin zum Strahlverlust kommt. Ein stabiler *Bunch-to-Bucket-Transfer* zwischen zwei Ringen ist daher sehr wichtig für FAIR und ist das Thema, welches im Rahmen dieser Doktorarbeit untersucht wird. Obwohl bereits zwischen SIS18 und ESR ein B2B-Transfer realisiert wurde, so ist diese Lösung aufgrund verschiedener Einschränkungen nicht nutzbar für FAIR. Es liegt das alte GSI-Kontrollsystem, ein eventbasiertes System zu Grunde, welches in Zukunft vollständig durch das neue FAIR-Kontrollsystem ersetzt werden wird. Auch lässt sich die alte Lösung nicht mit dem White Rabbit Timing synchronisieren, was für das *FAIR B2B transfer system* obligatorisch ist. Des Weiteren unterstützt es nicht die *phase shift method* und ermöglicht auch keine komplexen Buckete-Füllmuster. Zu einem Strahltransfer über Targets ist es ebenfalls nicht in der Lage. Die Entwicklung eines *FAIR B2B transfer systems*, basierend auf der für FAIR geplanten technischen Infrastruktur, dazu zählen das FAIR Kontrollsystem und das *FAIR LLRF System* ist daher unbedingt erforderlich.

Diese Doktorarbeit stellt erstmals die konzeptionelle Realisierung des *FAIR B2B transfer system* vor. In den meisten Fällen wird der FAIR B2B-Transfer mit einem B2B-Injektions-Mittenversatz von unter  $\pm 1^\circ$  innerhalb der oberen Zeitgrenze von 10ms erreicht. Das *FAIR B2B transfer system* unterstützt die *phase shift method*, wie auch die *frequency beating method* und ist anpassungsfähig genug, um einen Transfer zwischen zwei Ringen mit beliebigen Umfangszahlenverhältnis zu ermöglichen. Es ist möglich, verschiedenen B2B-Transfers zur gleichen Zeit auszuführen. Beispielsweise kann der B2B-Transfer vom SIS18 zum SIS100 zur gleichen Zeit stattfinden, wie der B2B-Transfer vom ESR zum CRYRING. Auch können verschiedenen Ionensorten von einem zum anderen Maschinenzyklus transferiert werden. Das *FAIR B2B transfer system* ist in der Lage, einen Transfer zwischen zwei Ringen auch über das Antiprotonen-Target, den Fragmentseparator oder den Suprafragmentseparator durchzuführen. Es können verschiedenen komplexe Bucket-Füllmuster berücksichtigt werden. Außerdem hat das *FAIR B2B transfer system* eine Schnittstelle zum FAIR-Maschinenschutzsystem, welches den SIS100 und die nachgeschalteten Beschleuniger und Experimente vor Schaden zu bewahren.

Für die *phase shift method* wurden verschiedene Modulationsmuster für die HF-Frequenzmodulation des SIS18-Strahls detailliert analysiert und anhand mehrerer Kriterien bewertet. Entsprechend der strahldynamischen Analyse wird die maximal mögliche Frequenzmodulation durch die Randbedingung beim *momentum shift* eingeschränkt. Die erste Ableitung der HF-Frequenzmodulation muss stetig und klein genug sein, um eine ausreichende Größe der umlaufenden *buckets* zu garantieren. Ein kleiner Wert der zweiten Ableitung garantiert, dass sich die synchrone Phase langsam genug ändert, damit der Strahl folgen kann. Das spiegelt sich auch im adiabatischen Parameter wieder. Um einen *bucket*-Fläche von größer 80% und einen adiabatischen Parameter von kleiner  $10^{-4}$  für den SIS18 200 MeV/u  $U^{28+}$  Strahl garantieren zu können, muss  $|\Delta f_{rf}|$  kleiner als 8.137 kHz sein und  $|\frac{d\Delta f_{rf}}{dt}|$  muss stetig und kleiner als 95 Hz/ms sein.  $|\frac{d^2\Delta f_{rf}}{dt^2}|$  muss kleiner als 70 Hz/ms<sup>2</sup> sein. Für den SIS18 4 GeV  $H^+$  Strahl, muss  $|\Delta f_{rf}|$  kleiner als 283 Hz sein und  $|\frac{d\Delta f_{rf}}{dt}|$  muss stetig und kleiner als 1.9 Hz/ms sein.  $|\frac{d^2\Delta f_{rf}}{dt^2}|$  muss kleiner als 0.2 Hz/ms<sup>2</sup> sein. Hinsichtlich dieser Anforderungen wurden ein sinusförmiges und parabelförmiges HF-Frequenzmodulationsprofil mit fester Zeitdauer überprüft für den SIS18  $U^{28+}$  Strahl. Beide Modulationsprofile erfüllen die Anforderungen und halten den Strahl stabil. Dennoch ist der adiabatische Parameter bei der sinusförmigen Modulation kleiner als bei der parabelförmigen Modulation. Folglich sollte die sinusförmige Modulation bei der *phase shift method* bevorzugt werden. Die sinusförmige HF-Frequenzmodulation im SIS18 für 200 MeV/u  $U^{28+}$  benötigt 7 ms und die sinusförmige HF-Frequenzmodulation im SIS18 für 4 GeV  $H^+$  benötigt circa 50 ms für eine Phasenverschiebung jeweils um  $\pi$ .

In Ergänzung zu den strahldynamischen Analysen, wurden zwei Messaufbauten errichtet. Der erste Messaufbau diente dazu, das WR-Netzwerk für den B2B-Transfer zu charakterisieren. Nach diesem Messergebnis, ist die zulässige Anzahl von WR-Switch-Layer für den B2B-Transfer nicht nur von der Obergrenze der Latenzzeit ab (e.g. 400 ms), sondern auch von der tolerierbaren Frame-Error-Rate (FER) des B2B-Transfer-Systems. Wenn keine Vorwärtsfehlerkorrektur für das B2B-Netzwerk verwendet wird, ist die Anzahl der zulässigen WR-Switches hauptsächlich durch die FER bestimmt. Unter der Annahme, dass der Verlust von einem Frame pro **zwei** Monat noch akzeptable ist, sind maximal 38 WR-Switches zulässig zwischen Data Master (DM) und den zugehörigen SCUs und maximal 8 WR-Switches direkt zwischen den SCUs, die dem B2B zugeordnet sind. **Wird** eine Vorwärtsfehlerkorrektur für das B2B-Netzwerk verwendet, so ist die Anzahl der zulässigen WR-Switches durch die noch tolerierbare Latenzzeit bestimmt. In diesem Fall, sind dann 67 WR-Switches zwischen den für das B2B zugehörigen SCUs und DM erlaubt und 13 WR-Switches direkt zwischen den SCUs, die dem B2B zugeordnet sind. Der zweite Messaufbau diente dazu, die Firmware für das *B2B transfer system*, die auf einer *Soft-CPU* (*LatticeMicro32*) in der SCU ausgeführt wird, zu evaluieren. Gemessen wurden die Laufzeiten für die einzelnen Tasks in der Firmware. Es wurde nachgewiesen, dass die Firmware auf dem LatticeMicro32 in der SCU die Anforderungen an die Timing-Bedingungen erfüllt, wenn der zugehörige *System-on-Chip bus* nicht zur gleichen Zeit mit anderen Anwendung, die parallel zur B2B-Firmware laufen belegt ist.

Des Weiteren wurden die Auswirkung der Fehlerfortpflanzung durch die Messunsicherheit (z.B. die Phasenmessgenauigkeit von  $\pm 0.1^\circ$ , der BuTiS Clock-Jitter von die 100 ps und die Messgenauigkeit für den Zeitstempel von 1 ns) für die Zeit **bis**

zum *phase alignment* in allen FAIR-Anwendungsfällen im Rahmen dieser Doktorarbeit überprüft. Der B2B Mittenversatz bei Injektion verschlechtert sich durch die zeitlichen Unsicherheiten bei der Bestimmung des Zeitpunkts des *phase alignment* in unterschiedlichem Grad. In einigen Anwendungsfällen verschlechtert sich der B2B Mittenversatz bei Injektion sehr deutlich. Beispielsweise verschlechtert sich der Mittenversatz um 37% für den Transfer von  $U^{28+}$  vom SIS18 in den SIS100. Trotz dieser Verschlechterung wird die Anforderung von kleiner  $\pm 1^\circ$  eingehalten. Daher ist die Messunsicherheit noch akzeptabel für das *FAIR B2B transfer system*. Zusätzlich wurden im Rahmen dieser Doktorarbeit auch die Genauigkeitsanforderungen an den Start des Synchronisationsfenster für alle FAIR-Anwendungsfälle überprüft. Der  $h=1$  B2B-Transfer vom SIS18 zum ESR stellt mit ca. 500 ns die härtesten Genauigkeitsanforderungen an den Beginn des Synchronisationsfensters.

Außerdem wurden verschiedenen Trigger-Szenarien für den SIS18 Extraktions- und den SIS100 Injektions-Kicker-Magnet untersucht. Die neuen Extraktions-Kicker-Magnete, sind in zwei Tanks verteilt. Die Kicker-Magnete jedes Tanks können gleichzeitig gezündet werden, wenn die Bunchlücke mindestens mindestens 25% der Kavitäten-HF-Periode beträgt. Die vier Kicker-Magnete in dem zweiten Tank, können nach einer festen Verzögerungszeit nach dem Zünden der fünf Kicker-Magnete im ersten Tank für alle Ionensorten ausgelöst werden, wenn die Bunchlücke mindestens 25% der Kavitäten-HF-Periode beträgt. Die sechs SIS100 Injektions-Kicker-Magneten sind gleichmäßig in einem Tank verteilt. Sie können unverzüglich für alle Ionensorten gezündet werden, wenn die Bunchlücke mindestens 35% der Kavitäten-HF-Periode beträgt.

Zum Abschluß wurde das *FAIR B2B transfer system* unter Anwendung der *frequency beating method* für alle FAIR-Anwendungsfälle dargestellt. Es wurde gezeigt, dass für alle Primärstrahl-Transfers in den FAIR-Anwendungsfällen, bei Injektion einen B2B Mittenversatz von besser  $\pm 1^\circ$  innerhalb der erforderlichen Transferzeit von 10 ms erreicht wird, weil das Zahlenverhältnis der Umfänge der beiden Ringe ganzzahlig oder nahezu ganzzahlig ist. Entwicklungsbedarf besteht noch beim Ionentransfer von Sekundärstrahlen, wie sie vom Antiprotonen-Target, dem Fragmentseparator oder dem Suprafragmentseparator erzeugt werden. Hier besteht das Problem, dass das Verhältnis der Energien zwischen Primär- und Sekundärstrahl sich stark unterscheiden. Für den Transfer von exotischen Nuklide vom SIS100 zum CR über den Suprafragmentseparator mit 1.5 GeV/u Primärstrahlenergie und 740 MeV/u Sekundärstrahlenergie, beträgt der B2B Injektions-Mittenversatz zwar zufällig nur  $\pm 2.1^\circ$ , für den Antiprotonen B2B-Transfer vom SIS100 zum CR über das Antiprotonen-Target und den seltene Isotopen Strahltransfer vom SIS18 zum ESR über den Fragmentseparator, ist der B2B Mittenversatz aber schon größer als  $\pm 40^\circ$  und damit weit außerhalb der Spezifikation.

Die vorliegende Doktorarbeit stellt die wesentlichen Untersuchungsergebnisse für den *FAIR B2B transfer system*, aus Sicht der Strahldynamik, Timing Anforderung und Kicker-Auslösung vor. Dennoch bleiben weitere Untersuchungsaufgaben, die für den finalen Anlagenbetrieb notwendig sind offen. Dazu zählen:

- Die Synchronisation im Mikrosekundenbereich des Antiprotonenstrahls mit dem magnetischen Horn nach dem Antiprotonen-Target.
- Die Synchronisation zwischen dem SIS100 Bunchkompressor und der Strahl-extraktion.



- In einige FAIR-Anwendungsfällen ist für den Transfer des Sekundärstrahls der B2B Injektions-Mittenversatz größer als  $\pm 40^\circ$ . Für diese Anwendungsfälle muss überprüft werden, ob der B2B-Transfer unter Zuhilfenahme von speziellen Strahlaufspeicherung-Methoden ???oder Strahlakkumulation-Methoden wie Beispielsweise *barrier bucket method* oder *unstable point accumulation method* gelingt.

Das *FAIR B2B transfer system*, das in dieser Doktorarbeit vorgestellt wird, ist anwendbar für alle FAIR-Anwendungsfälle. Dennoch gibt es noch Verbesserungspotential. Für die *phase shift method* muss die HF-Frequenzmodulation sehr langsam erfolgen, damit der Strahl der Frequenzänderung folgen kann (z.B. 7 ms/50 ms sinusförmige Modulation für den SIS18  $U^{28+}/H^+$  Strahl). Um Bunche sobald wie möglich in Buckets transferieren zu können, kann mit der Phasenverschiebung bereits auf der Beschleunigungsrampe begonnen werden. Zu einem definierten Zeitpunkt während des Beschleunigungsprozesses wird die Phasendifferenz zwischen den beiden HF-Systemen der Quell- und Zielmaschine unter Zuhilfenahme eines *synchronisation reference signal* ermittelt. Die Phasendifferenz auf dem *rf flattop* wird über eine Look-Up-Table aus den Phasendifferenzen, die zu definierten Zeitpunkten auf der Rampe gewonnen wurden ermittelt. Daraus lässt sich die benötigte HF-Frequenzmodulation berechnen. Diese wird der ursprünglichen Frequenzrampe überlagert. Mit der so entstandenen Frequenzrampe, wird die gewünschte Phasendifferenz dann automatisch erzielt, wenn die HF-Frequenz von Quell- und Zielmaschine das *rf flattop* erreichen.

# Glossaries, Abbreviations and Symbols



# Glossary

accuracy	Deviation between the theoretically calculated start time of the synchronization window and the actual observed start time
B2B transfer master	Responsible for the data collection of two ring accelerators, the data calculation, the data redistribution and the B2B transfer status check
B2B target SCU	Collects the predicted phase of the target synchrotron and transfers it to the source synchrotron
B2B source SCU	Works as the B2B transfer master
batch	A train of bunches circulating along a synchrotron to be transferred to buckets
best estimate time of alignment	Fine time for the alignment of two RF Reference Signals
bucket indication signal	Time indication of a dedicated bucket passing on the virtual rf cavity of the target synchrotron, when it is correct phase aligned with the rf system of the source synchrotron for the bunch-to-bucket injection
bucket pattern	Rules for the buckets to be filled
bucket area factor	Ratio of bucket size of a running bucket to a stationary bucket
bucket size	Area in longitudinal phase space plane enclosed by the bucket
bucket height	Maximum momentum deviation of the rf bucket

bunch	Collection of particles captured within one rf bucket
bunch gap	Area without any bunches in a batch
Cavity DDS	Cavity DDS provides rf signal for cavities
circumference ratio	Ratio of the circumference for synchrotrons of different size
coarse synchronization	Bunches are transferred into buckets with the bunch-to-bucket center mismatch smaller than the upper bound
extraction kicker	Diverts a circulating beam to leave a synchrotron
fine synchronization	Bunches are transferred into correct buckets
frame transfer latency	The time interval between the frame reception and sending
Group DDS	DDS module that generates an phase measurement signal for a group of cavities
harmonic number	Integer ratio between the rf frequency and the revolution frequency
injection kicker	Merges one beam into a circulating beam in a synchrotron
kicker fall time	A period of time of kicker magnet to reduce to zero magnetic field
kicker flat-top	A period of time of kicker magnet with a stable magnetic field
kicker rise time	A period of time for kicker magnet to reach a stable magnetic field
longitudinal emittance	Area occupied by a bunch in the longitudinal phase space plane

lost frame	The difference between the sent packets and the received packets
machine cycle	One complete operation cycle of a machine, i.e. injection, ramp up, flattop, ejection and ramp down
measurement uncertainty	A non-negative parameter characterizing the dispersion of the values attributed to a measured quantity
misordered frame	The number of misordered packets arriving out of sending sequence
phase measurement signal	Harmonic or subharmonic signal generated by the Group DDS and transmitted to the individual rf station as a reference signal
probable time range of alignment	Range within which the fine alignment lies because of the propagation of the uncertainty
revolution frequency ratio	Ratio of the revolution frequencies for synchrotrons of different size
running rf bucket	Rf system provides a region in the longitudinal phase space, within which all particles oscillate around the synchronous particle and stay together with energy gain/loss per turn
stationary rf bucket	Rf system provides a region in the longitudinal phase space, within which all particles oscillate around the synchronous particle and stay together without energy gain/loss per turn (short: bucket)
synchronization reference signal	Shared synchronous reference signal at each supply room (same frequency and in phase)
synchronization frequencies	An integer multiple of the derived rf frequency, which is a fraction of the revolution frequency. It is used for the phase alignment of the two rf systems

synchronous particle	A particle who always sees a constant rf phase at the rf cavity
synchrotron motion	Oscillation of asynchronous particles around the synchronous particle
T0 incidents	First positive zero-crossings of BuTiS C2 clocks after every BuTiS T0 edge
timing frame	A specific Ethernet frame with 110 byte frame length, which contains one timing message
Trigger SCU	Production of the trigger signal for kicker electronics
tune	Number of particle trajectory oscillations during one revolution in the ring (transverse and longitudinal)
virtual rf cavity	A virtual position around the ring, to which the phase measurement signal corresponds

# Abbreviations

AGS	Alternating Gradient Synchrotron at BNL
API	Application Programming Interface
B2B	Bunch-to-bucket
BER	Bit Error Rate
BI	Beam Instrumentation
BNL	Brookhaven National Laboratory
CCS	Central Control System
CERN	Conseil Européen pour la Recherche Nucléaire
CM	Clock Master
CR	Collector Ring at GSI
CSCO	Common Systems Control Systems
CSRe	Cooler Storage Ring experimental ring at IMP
CSRm	Cooler Storage Ring main ring at IMP
DDS	Direct Digital Synthesizer
DM	Data Master
DSP	Digital Signal Processor
ESR	Experimental Storage Ring at GSI
FAIR	Facility for Antiproton and Ion Research at GSI
FEC	Front End Controller

## Abbreviations

---

FER	Frame Error Rate
Fermilab	Fermi National Accelerator Laboratory
FESA	Front-End software Architecture
FLR	Frame Loss Rate
FPGA	Field Programmable Gate Array
FRS	Fragment Separator
GCD	Greatest Common Divisor
GMT	General Machine Timing
GSI	GSI Helmholtzzentrum für Schwerionen- forschung
GUI	Graphical User Interface
HESR	High Energy Storage Ring at GSI
HIRFL	Heavy Ion Research Facility at IMP
IMP	Institute of Modern Physics
J-PARC	Japan Proton Accelerator Complex
LEIR	Low Energy Ion Ring at CERN
LHC	Large Hadron Collider at CERN
LLRF	Low-level RF
LSA	LHC Software Architecture
MM	Management Master
MPS	Machine Protection System
MR	Main Ring at J-PARC
PAM	Phase Advance Measurement module
PAP	Phase Advance Prediction module
pbar	antiproton bar

PBHV	Primary Beam High Voltage
PBRF	Primary Beam Radio Frequency
PC	Personal Computer
PCM	Phase Correction Module
PS	Proton Synchrotron at CERN
PSB	Proton Synchrotron Booster at CERN
PSM	Phase Shift Module
RCS	Rapid Cycle Synchrotron at J-PARC
RHIC	Relativistic Heavy Ion Collide at BNL
RIB	Rare Isotope Beams
SBES	Experimentierspeicherring ESR
SCU	Scalable Control Unit
SFC	Sector Focusing Cyclotron at IMP
SHE-P	SHE-Physik
SIS100	SchwerIonen Synchrotron (100 Tm magnetic rigidity) at GSI
SIS18	SchwerIonen Synchrotron (18 Tm magnetic rigidity) at GSI
SIS300	SchwerIonen Synchrotron (300 Tm magnetic rigidity) at GSI
SM	Settings Management
SPS	Super Proton Synchrotron at CERN
SR	Signal Reproduction module
SSC	Separated Sector Cyclotron at IMP
TM	Timing Master

## Abbreviations

---

TOF	Time-Of-Flight
UNILAC	Universal Linear Accelerator at GSI
VLAN	Virtual LAN
WR	White Rabbit



# Symbols

$p$	Particle momentum
$R$	Average orbit radius
$L$	Orbit length
$\beta$	Relative speed to the speed of light
$c$	Speed of the light
$\gamma$	Relativistic factor, which measures the total particle energy, $E$ , in units of the particle rest energy, $E_0$
$E$	Total particle energy
$E_0$	Particle rest energy
$\alpha_p$	Momentum compaction factor
$\eta$	Phase-slip factor
$q$	Charge of a particle
$\alpha_b$	Bucket area factor
$\omega_s$	Angular synchrotron frequency
$B$	Magnetic field
$\rho$	Bending radius of a particle immersed in a magnetic field $B$
$h_{rf}^X$	Cavity harmonic number of a specified synchrotron

$h_{rev}^X$	Harmonic number of the revolution frequency of a specific synchrotron, which is defined as the first harmonic
$f_{syn}^X$	Synchronization frequency
$h_{syn}^X$	Harmonic number of the synchronization frequency of a specific synchrotron
$\varepsilon$	Adiabaticity parameter
$Q_{x/y}$	Horizontal/vertical tune
$Q'_{x/y}$	Horizontal/vertical chromaticity
$\Delta Q_{x/y}$	Horizontal/vertical tune shift
$T_w$	Length of the synchronization window
$t_{bucket}$	Bucket delay for a specific bucket pattern
$t_{TOF}$	Time-of-Flight between two ring accelerators
$t_{v-ext}$	Time corresponding to the distance between the virtual rf cavity and the extraction position of the source synchrotron
$t_{v-inj}$	Time corresponding to the distance between the virtual rf cavity and the injection position of the target synchrotron
$t_{ext}$	Extraction kicker delay
$t_{inj}$	Injection kicker delay
$t_{diff\_sync}$	Goal time difference between the synchronization frequencies of two ring accelerators in the format of time
$\phi^X$	Measured phase deviation between the synchronization frequency and the synchronization reference signal of the synchrotron X
$\varphi^X$	Measured phase deviation between the phase measurement signal and the synchronization reference signal of the synchrotron X

$\varphi_0^X$	Initial value of the phase deviation between the phase measurement signal and the synchronization reference signal of the synchrotron X
$T_{sample\_PAM}$	Measurement sampling period of the phase deviation measurement by the PAM module
$\psi^X$	Extrapolated phase advance between the phase measurement signal and the synchronization reference signal of the synchrotron X
$T_{sample\_PAP}$	Extrapolation sampling period of the phase extrapolation by the PAP module
$\psi_0^X$	Phase advance extrapolated by the PAP module at $t_\psi^X$ of the X synchrotron.
$t_\psi^X$	Timestamp corresponding to the extrapolated phase advance $\psi^X$
$f_{normalized}$	Normalized rf frequency modulation profile, preloaded from SM
$f_{actual}$	Actual rf frequency modulation profile, calculated by PSM
$t_{delay}$	Delay compensation for the TOF, all propagation delays, the kicker preparation time and the bucket delay
$t_w$	Start of the synchronization window, calculated by B2B source SCU
$t_{v\_emg}$	Time corresponding to the distance between the virtual rf cavity and the emergency extraction position of SIS100
$t_{emg}$	Extraction kicker delay of SIS100 for the emergency kick
$t_{align}$	Best estimate of alignment of zero crossing points of phase measurement signals of source and target synchrotrons
$\delta t_{align}$	Uncertainty of the best estimate of alignment of zero crossing points of phase measurement signals of source and target synchrotrons

$\delta\psi_0^X$	Uncertainty of the extrapolated phase of the synchrotron X in the phase domain
$\delta t_\psi^X$	Uncertainty of the measured timestamp
$t_{w\_rect}$	Rectified start of the synchronization window, calculated by B2B source SCU
$\delta t_{w\_rect}$	Uncertainty of the start of the synchronization window, calculated by B2B source SCU
$t_{B2B}$	Start time of the B2B transfer
$t_{rise}$	Kicker rise time.
$t_{gap}$	Bunch gap
$d_{tank1L-tank1R}$	Distance between the leftmost and the rightmost kicker magnets in the 1 <sup>st</sup> SIS18 tank
$d_{tank2L-tank2R}$	Distance between the leftmost and the rightmost kicker magnets in the 2 <sup>nd</sup> SIS18 tank
$d_{tank1R-tank2L}$	Distance between two tanks of the SIS18 extraction kicker
$d_{tank1L-tank2R}$	Distance from the leftmost to the rightmost of the SIS18 extraction/SIS100 injection kicker
$d_{tank1R-tank2R}$	Distance between the rightmost of the 1 <sup>st</sup> tank and the rightmost of the 2 <sup>nd</sup> tank of the SIS18 extraction kicker
$d_{tankL-tankR}$	Distance between the leftmost and the rightmost kicker magnets in the SIS100 tank
$\phi_s$	Synchronous phase
$f_{rf}$	Rf frequency
$h$	Harmonic number
$f_{rev}$	Revolution frequency
$f_{ref}$	Frequency of the synchronization reference signal

$f_{B2B}^X$	Frequency of the specified phase measurement signal for the phase advance measurement
$u$	Longitudinal accelerating voltage at rf cavity
$V_0$	Amplitude of the rf voltage
$m_0$	Rest mass
$C^X$	Circumference of the extraction/injection orbit of a specific synchrotron
$f_{rev}^X$	or $f_{h=1}^X$ . Revolution frequency of a specific synchrotron
$f_{rf}^X$	or $f_{h=cavity\_harmonic}^X$ . Cavity rf frequency of a specific synchrotron
$T$	Duration of rf frequency modulation for the phase shift method
$Y$	Greatest common divisor
$\phi_0^X$	Initial phase deviation between the synchronization frequency and synchronization reference signal of the synchrotron X
$\Delta\phi_{rf}$	Phase difference between two cavity rf frequencies of two ring accelerators
$\Delta\phi_{syn}$	Phase difference between two synchronization frequencies of two ring accelerators
$\Delta f_{syn}$	Rf frequency modulation on the synchronization frequency for the phase shift method, rf frequency detuning on the synchronization frequency for the frequency beating method
$\Delta f_{rf}$	Rf frequency modulation on the cavity rf frequency for the phase shift method, rf frequency detuning on the cavity rf frequency for the frequency beating method
$\sigma_{syn}$	Phase mismatch between two synchronization frequencies within the synchronization window

$\sigma_{rf}$	Phase mismatch between two cavity rf frequencies within the synchronization window
$T_{rev}^X$	Period of the revolution period of machine X
$T_{rf}^X$	Period of the cavity rf frequency of machine X
$f_{bucket}$	Rf frequency of the bucket indication signal
$k^X$	Slope of the phase deviation between the synchronization reference signal and a dedicated phase measurement signal of the synchrotron X
$\Delta\phi_{syn\_0}$	Phase difference between two synchronization frequencies of two ring accelerators at time $t_{\psi}^X$
$\Delta\phi_{goal}$	Goal phase difference between the synchronization frequencies of two ring accelerators
$\Delta\phi_{adjust}$	Required phase adjustment for the phase alignment on the synchronization frequency
$\Delta\phi_{shift}$	Required phase shift for the Group DDS with the synchronization frequency
$\Delta\phi_{shift\_imp}$	Implemented phase shift for the Group DDS with the revolution frequency
$T_{wait}$	Waiting time for the phase matching of the frequency beating method

# Appendix A

## FAIR B2B Transfer Related Timing Frames

## APPENDIX A. FAIR B2B TRANSFER RELATED TIMING FRAMES

Table A.1: B2B timing frames

No	Frame Name	Event ID	Priority	Source	Destination
1	CMD_START_B2B		7	DM	B2B source and target SCUs
2	TGM_PHASE_TIME		6	B2B target SCU	B2B source SCU
3	TGM_SYNC_WIN		6	B2B source SCU	DM
4	CMD_SYNC_WIN		7	DM	BI, source and target Trigger SCUs
5	TGM_PHASE_JUMP		6	B2B source SCU	B2B target SCU
6	TGM_PHASE_CORRECTION		6	B2B source SCU	source Trigger SCU
7	TGM_KICKER_TRIGGER_TIME_S		6	source Trigger SCU	B2B source SCU
8	TGM_KICKER_TRIGGER_TIME_T		6	target Trigger SCU	B2B source SCU
9	TGM_B2B_STATUS		6	B2B source SCU	DM
10	CMD_B2B_STATUS		7	DM	BI
11	TGM_B2B_ERROR		7	B2B source SCU	DM
No	Content	Description			
1	64 bits timestamp(event execution)	Begin of the B2B transfer process			
2	16 bits phase advance and 64 bits slop (param)	Transfer of the phase advance and the slop			
3	64 bits timestamp (param)	Transfer the start of the synchronization window			
4	64 bits timestamp (event execution)	Indication the start of the synchronization window			
5	16 bits the expected jumped phase (param)	Indication the jumped phase for the empty target machine			
6	16 bits phase correction (param)	Target revolution frequency reproduction			
7	$2 \times 64$ bits timestamp (param)	Timestamps of trigger and firing of extraction kicker			
8	$2 \times 64$ bits timestamp (param)	Timestamps of trigger and firing of injection kicker			
9	64 bits timestamp + 1 bit (param)	The actual beam extraction time and the status of the B2B system			
10	64 bits timestamp (param)	The actual beam extraction time			
11	4 bits (param)	The error information			



## Appendix B

### Timing Frames Transfer for the FAIR B2B Transfer System

APPENDIX B. TIMING FRAMES TRANSFER FOR THE FAIR B2B TRANSFER SYSTEM

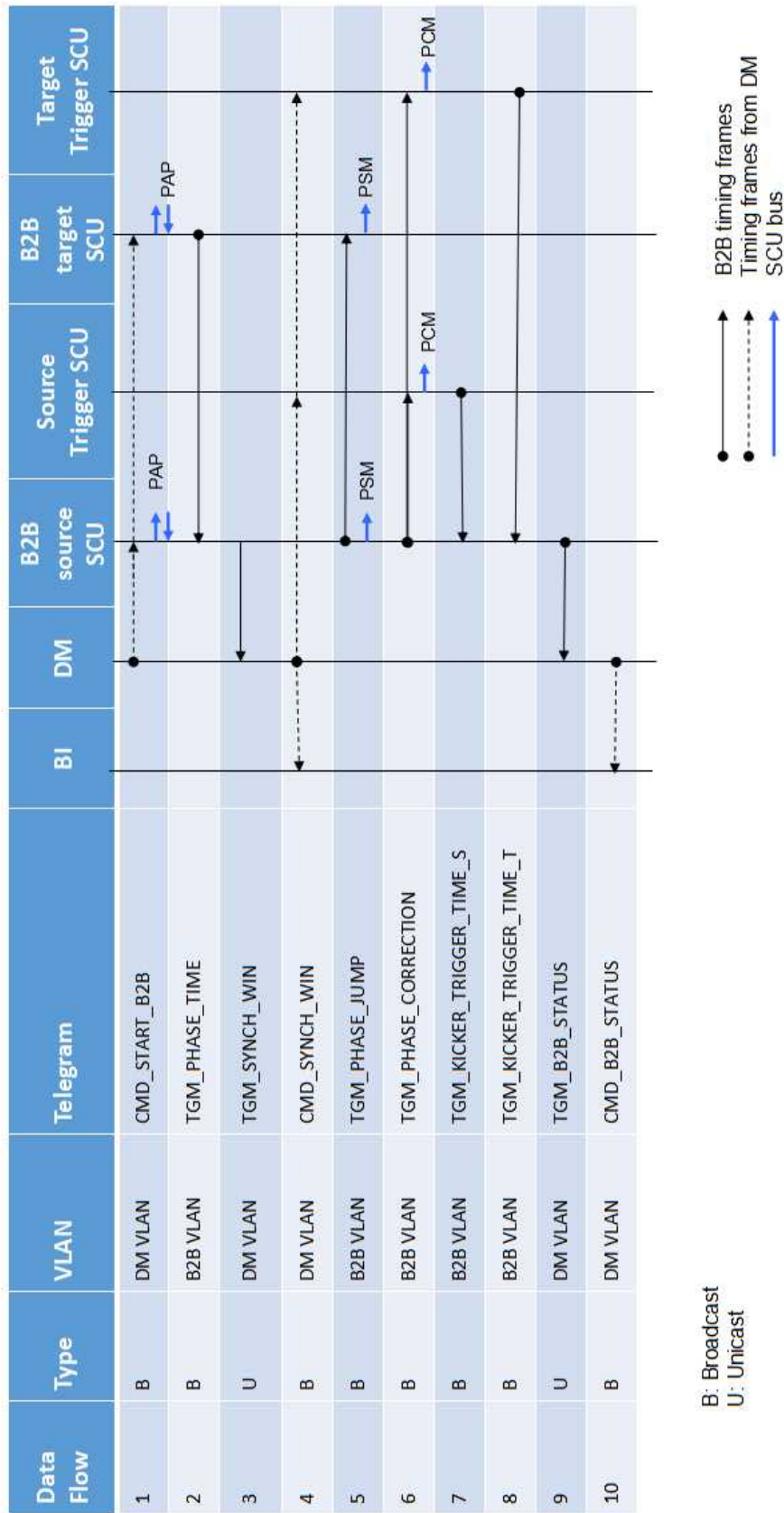


Figure B.1: Timing frames transfer for the B2B transfer

# Appendix C

## Parameters of FAIR B2B Transfer Use Cases

### C.1 Parameters of the B2B Transfer from SIS18 to SIS100

		Proton		Heavy Ion $U^{28+}$	
	Unit	SIS18 Ext	SIS100 Inj	SIS18 Ext	SIS100 Inj
Design orbit	m	216.72	1083.6	216.72	1083.6
$C_{SIS18} : C_{SIS100}$		5		5	
Ext kinetic energy	MeV/u	4000		200	
Inj kinetic energy	MeV/u		4000		200
h		1	10(1×4)	2	10(2×4)
$f_{rf}$	MHz	1.359358	2.718715	1.572536	1.572536
$T_{rf}$	μs	0.736	0.368	0.636	0.636
$f_{rev}$	MHz	1.359358	0.271872	0.786268	0.157254
$T_{rev}$	μs	0.736	3.678	1.272	6.359
Max $\Delta p/p$		±0.008	±0.01	±0.008	±0.01
$\Delta R/R$		±0.8 × 10 <sup>-4</sup>		±2.4 × 10 <sup>-4</sup>	
$\eta = \frac{1}{\gamma^2} - \alpha_p$		0.026		0.647	
$\gamma_t$		10		5.8	
$\alpha_p$		0.010		0.030	
$\beta$		0.982	0.982	0.568	0.568
$\gamma$		5.294	5.294	1.215	1.215
$Q_x$		4.17		4.17	
$Q_y$		3.4		3.4	
$Q'_x$		-7.5		-6.5	
$Q'_y$		-4.4		-4.1	
		Injection four times		Injection four times	

Table C.1: Parameters related to the B2B transfer from the SIS18 to the SIS100

## C.2 Parameters of the B2B Transfer from SIS18 to ESR

		Proton/Heavy Ion		Heavy Ion	
	Unit	SIS18 Ext	ESR Inj	SIS18 Ext	ESR Inj
Design orbit	m	216.72	108.36	216.72	108.36
Inj orbit	m		108.36 +0.15		108.36 +0.15
$C_{SIS18} : C_{ESR}$		1.997		1.997	
Ext kinetic energy	MeV/u	550		30	
Inj kinetic energy	MeV/u		400		30
h		1	1	4	2
$f_{rf}$	MHz	0.989756	1.976777	1.373201	1.371302
$T_{rf}$	$\mu$ s	1.010	0.506	0.728	0.879
$f_{rev}$	MHz	0.989756	1.976777	0.343300	0.685651
$T_{rev}$	$\mu$ s	1.010	0.506	2.913	1.458
$\Delta p/p$ compared with design orbit			1%		1%
$\Delta R/R$			0.138%		0.138%
$\eta = \frac{1}{\gamma^2} - \alpha_p$		0.480	0.310	0.909	0.759
$\gamma_t$		10	2.357	5.8	2.357
$\alpha_p$		0.010	0.18	0.030	0.18
$\beta$		0.715	0.715	0.248	0.248
$\gamma$		1.429	1.429	1.032	1.032
		Accumulation beam in injection orbit		Accumulation beam in injection orbit	

Table C.2: Parameters related to the B2B transfer from the SIS18 to the ESR

### C.3 Parameters of the B2B Transfer from SIS18 to ESR via the FRS

		Heavy Ion Beam	Rare Isotope Beam
	Unit	SIS18 Ext	ESR Inj
Design orbit	m	216.72	108.36
Inj orbit	m		108.36 +0.15
$C_{SIS18} : C_{ESR}$		1.997	
Ext kinetic energy	MeV/u	550	
Inj kinetic energy	MeV/u		400
h		1	1
$f_{rf}$	MHz	1.076965	1.976777
$T_{rf}$	$\mu$ s	0.929	0.506
$f_{rev}$	MHz	1.076965	1.976777
$T_{rev}$	$\mu$ s	0.929	0.506
$\Delta p/p$ compared with design orbit			1%
$\Delta R/R$			0.138%
$\eta = \frac{1}{\gamma^2} - \alpha_p$		0.366	0.310
$\gamma_t$		5.8	2.357
$\alpha_p$		0.030	0.18
$\beta$		0.778	0.715
$\gamma$		1.590	1.429
		One time injection	

Table C.3: Parameters related to the B2B transfer from the SIS18 to the ESR via the FRS

## C.4 Parameters of the B2B Transfer from ESR to CRYRING

		Proton/Antiproton		Heavy Ion	
	Unit	ESR Ext	CRYRING Inj	ESR Ext	CRYRING Inj
Design orbit	m	108.36	54.18	108.36	54.18
Ext orbit	m	108.36 +0.15		108.36 +0.15	
$C_{ESR} : C_{CRYRING}$		2.003		2.003	
Ext kinetic energy	MeV/u	30		4-10	
Inj kinetic energy	MeV/u		30		4-10
h		1	1	1	1
$f_{rf}$	MHz	0.685651	1.373200	0.254354- 0.400885	0.509507- 0.802879
$T_{rf}$	$\mu$ s	1.458	0.728	3.932- 2.494	1.963- 1.246
$f_{rev}$	MHz	0.685651	1.373200	0.254354- 0.400885	0.509507- 0.802879
$T_{rev}$	$\mu$ s	1.458	0.728	3.932- 2.494	1.963- 1.246
$\eta = \frac{1}{\gamma^2} - \alpha_p$		0.759		0.798-0.812	
$\gamma_t$		2.357		2.357	
$\alpha_p$		0.18		0.18	
$\beta$		0.248	0.248	0.092-0.145	0.092-0.145
$\gamma$		1.032	1.032	1.004-1.011	1.004-1.011
		One time injection		One time injection	

Table C.4: Parameters related to the B2B transfer from the ESR to the CRYRING

## C.5 Parameters of the B2B Transfer from CR to HESR

		Proton→ Antiproton		Heavy Ion→ RIB	
	Unit	CR Ext	HESR Inj	CR Ext	HESR Inj
Design orbit	m	221.45	575	221.45	575
$C_{HESR} : C_{CR}$		2.597		2.597	
Ext kinetic energy	GeV/u	3		0.74	
Inj kinetic energy	GeV/u		3		0.74
h		1	1	1	1
$f_{rf}$	MHz	1.316775	0.507131	1.124408	0.433043
$T_{rf}$	$\mu$ s	0.759	1.972	0.889	2.309
$f_{rev}$	MHz	1.316775	0.507131	1.124408	0.433043
$T_{rev}$	$\mu$ s	0.759	1.972	0.889	2.309
Max $\Delta p/p$		$\pm 3\%$		$\pm 1.5\%$	
$\eta = \frac{1}{\gamma^2} - \alpha_p$		-0.011		0.178	
$\gamma_t$		3.85		2.711	
$\alpha_p$		0.067			
$\beta$		0.972	0.972	0.830	0.830
$\gamma$		4.221	4.221	1.794	1.794
		100 times Injection per 10 seconds		100 times Injection per 10 seconds	

Table C.5: Parameters related to the B2B transfer from the CR to the HESR

## C.6 Parameters of the B2B Transfer from SIS100 to CR

		Proton→ Antiproton		Heavy Ion→ RIB	
	Unit	SIS100 Ext	CR Inj	SIS100 Ext	CR Inj
Design orbit	m	1083.6	221.45	1083.6	221.45
$C_{SIS100} : C_{CR}$		4.893		4.893	
Ext kinetic energy	GeV/u	28.8		1.5	
Inj kinetic energy	GeV/u		3		0.74
h		5(1 bunch)	1	2(1 bunch)	1
$f_{rf}$	MHz	1.383509	1.316778	0.511628	1.124408
$T_{rf}$	$\mu$ s	0.723	0.759	1.955	0.889
$f_{rev}$	MHz	0.276702	1.316778	0.255814	1.124408
$T_{rev}$	$\mu$ s	3.614	0.759	3.909	0.889
Max $\Delta p/p$		$\pm 3\%$		$\pm 1.5\%$	
$\beta$		0.9995	0.972	0.924	0.830
$\gamma$		31.918	4.221	2.610	1.794
		One time injection		One time injection	

Table C.6: Parameters related to the B2B transfer from the SIS100 to the CR



## **Appendix D**

### **Parameters of the FAIR B2B Transfer System from Settings Management**

## APPENDIX D. PARAMETERS OF THE FAIR B2B TRANSFER SYSTEM FROM SETTINGS MANAGEMENT

Table D.1: Parameters for the B2B transfer provided by SM

Parameter	Destination	Usage
$f_{syn}^X$	B2B source SCU	Start of synchronization window calculation
$f_{syn}^{REF}$	B2B source SCU	Phase advance extrapolation for PCM
Frequency of bucket indication signal	B2B source SCU $\Rightarrow$ SR B2B target SCU $\Rightarrow$ SR Trigger SCU $\Rightarrow$ SR	Bucket label signal production
$t_{delay}$ Delay compensation for TOF, all propagation and kicker preparation	B2B source SCU	Start of synchronization window calculation
Extraction kicker delay compensation	Trigger SCU $\Rightarrow$ TD	Extraction kicker trigger signal production
Injection kicker delay compensation	Trigger SCU $\Rightarrow$ TD	Injection kicker trigger signal production
Emergency kicker delay compensation	Trigger SCU $\Rightarrow$ TD	Emergency kicker trigger signal production
Goal time difference between two synchronization frequencies of two synchrotrons	B2B source SCU	Start of synchronization window calculation or phase correction calculation for PCM
$\Delta f$	B2B source SCU	Start of synchronization window calculation
Duration of rf frequency modulation for the phase shift method	B2B source SCU $\Rightarrow$ PSM B2B source SCU $\Rightarrow$ PSM	Start of synchronization window calculation and rf frequency modulation profile with certain duration T production
$\Delta f_{rf}$ , $\dot{\Delta f}_{rf}$ and $\ddot{\Delta f}_{rf}$	B2B source SCU $\Rightarrow$ PSM	Adiabatical rf frequency modulation profile production

# Appendix E

## Parameters of FAIR Kicker Magnets

Table E.1: Parameters of kicker magnets

Kicker	Units	Preparation time	Kicker rise time	Kicker fall time
SIS18 extraction kicker	9	5 us	90 ns	arbitrary
SIS100 injection kicker	6	5 us	130 ns	$\frac{1}{4}T_{rev}$
SIS100 extraction/emergency kicker	8	10 us	750 ns	arbitrary
CR injection/extraction kicker	9		320 ns	
ESR injection kicker	3		90 ns	

# Appendix F

## Configuration for the Test Setup

The project is kept on the git repository

[https://github.com/GSI-CS-C0/bel\\_projects/tree/lm32\\_B2B\\_merge](https://github.com/GSI-CS-C0/bel_projects/tree/lm32_B2B_merge).

In the test setup, the frame CMD\_START\_B2B uses the eventID of *0XDEADBEEF11111111* as an example and the frame TGM\_PHASE\_TIME uses the eventID of *0XDEADBEEF22222222* as an example and the frame TGM\_SYNC\_WIN uses the eventID of *0XDEADBEEF33333333* as an example.

### F.1 Configuration of the B2B source SCU

```
1 Login the B2B source SCU
2 # ssh root@scu_name.acc.gsi.de
3 Configure the ECA queue to storage the B2B frames CMD_B2B_START and
  TGM_PHASE_TIME
4 # saft-ecpu-ctl baseboard -c 0XDEADBEEF11111111 32 0 0
5 # saft-ecpu-ctl baseboard -c 0XDEADBEEF22222222 32 0 0
6 Configure one IO port as an input for the TTL signal of the SIS18 DS345
7 # saft-io-ctl baseboard B2 -o 0
8 Load the B2B source SCU firmware to the LM32
9 # lm32-ctl
10 # load B2B_main_src.elf
```

### F.2 Configuration of the B2B target SCU

```
1 Login the B2B target SCU
2 # ssh root@scu_name.acc.gsi.de
3 Configure the ECA queue to storage the B2B frames CMD_B2B_START
4 # saft-ecpu-ctl baseboard -c 0XDEADBEEF11111111 32 0 0
5 Configure one IO port as an input for the TTL signal of the SIS100 DS345
6 # saft-io-ctl baseboard B2 -o 0
7 Load the B2B target SCU firmware to the LM32
8 # lm32-ctl
9 # load B2B_main_trg.elf
```

### F.3 Configuration of the Trigger SCU

```
1 Login the Trigger SCU
2 # ssh root@scu_name.acc.gsi.de
3 Configure the ECA queue to storage the B2B frames TGM_SYNCH_WIN
4 # saft-ecpu-ctl baseboard -c 0XDEADBEEF33333333 32 0 0
5 Configure one IO port as an output port
6 # saft-io-ctl baseboard B2 -o 1
7 Configure ECA to produce a TTL signal at the output port, when the frame
  TGM_SYNCH_WIN is executed
8 # saft-B2B-triggerSCU baseboard 0XDEADBEEF33333333 B2
9 Load the Trigger SCU firmware to the LM32
10 # lm32-ctl
11 # load B2B.main.trigger.elf
```

### F.4 Configuration of the packETH

The configuration of the packETH is shown as follows.

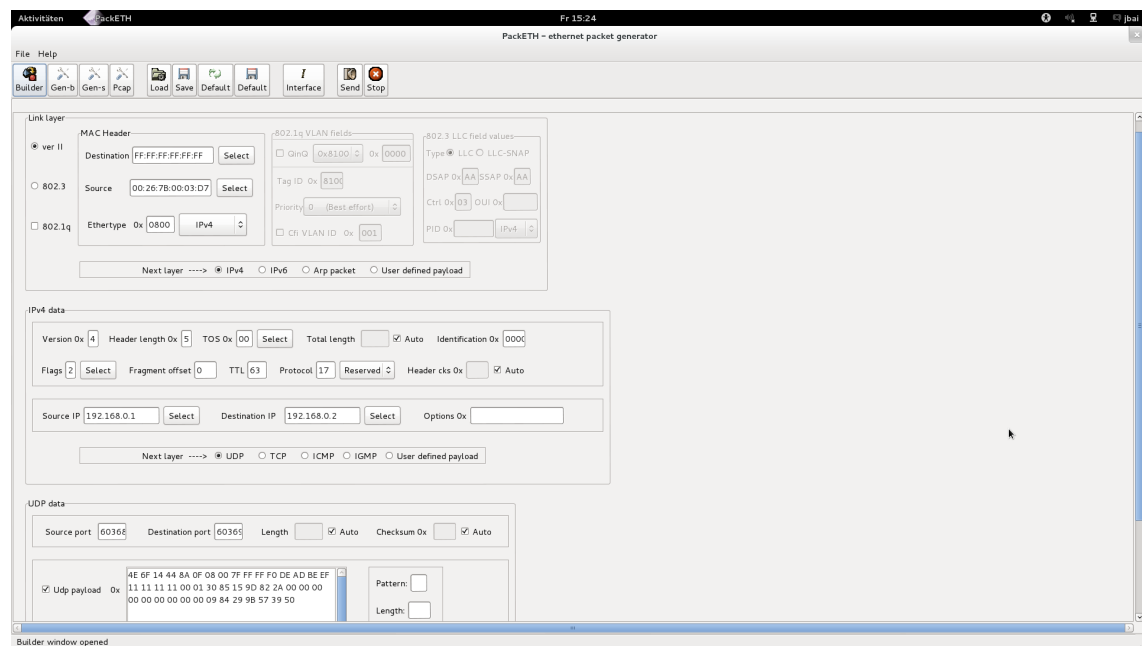


Figure F.1: The configuration of the packETH.

# List of Figures

1.1	Illustration of a bunch-to-bucket transfer. . . . .	2
1.2	Structure of the dissertation. . . . .	6
2.1	Longitudinal focusing of particles by an rf voltage ( $\eta > 0$ ). . . . .	10
2.2	Longitudinal motion of asynchronous particles in the longitudinal phase space plane ( $\eta > 0$ ). . . . .	10
2.3	A stationary rf bucket. . . . .	12
2.4	A running rf bucket. . . . .	13
2.5	Bunch-to-Bucket injection with a phase, energy or voltage error. . . .	14
2.6	A constant phase difference between two synchronization frequencies $f_{syn}^l$ and $f_{syn}^s$ when $\kappa = 5$ , $h_{rf}^s = 1$ and $h_{rf}^l = 10$ . . . . .	17
2.7	A periodically variable phase difference between two slightly different synchronization frequencies $f_{syn}^l$ and $f_{syn}^s$ when $\kappa = 2$ , $\lambda = -0.003$ , $h_{rf}^s = 2$ and $h_{rf}^l = 4$ . . . . .	19
2.8	A periodically variable phase difference between two synchronization frequencies $f_{syn}^l$ and $f_{syn}^s$ when $m = 26$ , $n = 10$ , $\lambda = -0.003$ , $h_{rf}^s = 1$ and $h_{rf}^l = 1$ . . . . .	20
2.9	An example for the phase shift method with a sinusoidal rf frequency modulation. . . . .	21
2.10	Illustration of the frequency beating method. . . . .	25
2.11	Schematic diagram of a kicker magnet. . . . .	27
2.12	Rise time, kicker flat-top and fall time of an extraction kicker. . . .	28
2.13	Rise time, kicker flat-top and fall time of an injection kicker for multiple batches injection. . . . .	29
3.1	Reference rf signal distribution system . . . . .	33
3.2	Local Cavity Synchronization . . . . .	34
4.1	Illustration of the B2B transfer from the SIS18 to the SIS100. . . . .	37
4.2	Frequency of the bucket indication signal equals to the revolution frequency of the target accelerator. . . . .	40
4.3	Frequency of the bucket indication signal equals to the synchronization frequency of the target accelerator. . . . .	40
4.4	Procedure for the B2B transfer within one acceleration cycle. . . . .	42
4.5	Phase deviation between the synchronization frequency and the synchronization reference signal. . . . .	43
4.6	Realization of the phase deviation measurement at one accelerator . .	46
4.7	Realization of the phase advance extrapolation at one accelerator . .	47

## LIST OF FIGURES

---

4.8	Synchronization of the extrapolated phase to the timestamp in one accelerator . . . . .	48
4.9	An example of the transfer path of the B2B timing frames in the WR network . . . . .	49
4.10	Normalized frequency and phase modulation profile and the actual profiles . . . . .	51
4.11	Transfer delay of the start of the synchronization window on the WR network. . . . .	52
4.12	Realization of the bucket label for the normal extraction and injection. . . . .	54
4.13	Realization of the maximum bunch spacing label for the emergency extraction. . . . .	55
4.14	Illustration of the kicker delay compensation when the bucket indication signal has the frequency of $f_{syn}^{try}$ . . . . .	57
4.15	Data flow of the B2B transfer system . . . . .	59
4.16	Current realization of the bunch-to-bucket transfer between the SIS18 and the ESR with the GSI control system. . . . .	61
5.1	Examples of rf frequency modulation. . . . .	66
5.2	First derivative of three cases. . . . .	67
5.3	Second derivative of three cases. . . . .	67
5.4	Phase shift modulation of three cases. . . . .	68
5.5	Maximum orbit length displacement of three cases. . . . .	69
5.6	Relative momentum shift of three cases. . . . .	70
5.7	Changes in synchronous phase of three cases. . . . .	71
5.8	Ratio of bucket areas of a running bucket to the stationary bucket of three cases. . . . .	71
5.9	Adiabaticity parameter of three cases. . . . .	72
5.10	Illustration of the rectification for the start of the synchronization window. . . . .	81
5.11	Illustration of the accuracy of the start of the synchronization window. . . . .	82
5.12	An overview of the Xena's Layer 2-3 test platform for the WR network. . . . .	83
5.13	Relation between the FER and the fiber connections for B2B Unicast and Broadcast traffics. . . . .	85
5.14	Connection between WR switches and the XenaBay of the test setup. . . . .	86
5.15	Maximum frame transfer latency for B2B Unicast frames. . . . .	88
5.16	Maximum frame transfer latency for B2B Broadcast frames. . . . .	89
5.17	Flowchart of the B2B source SCU. . . . .	92
5.18	Flowchart of the B2B target SCU. . . . .	94
5.19	Flowchart of the B2B Trigger SCU. . . . .	95
5.20	Time constraints of the B2B transfer system. . . . .	97
5.21	The schematic diagram of the controls and pulse electronics of the extraction kicker magnets in the SIS18 2 <sup>nd</sup> tank. . . . .	98
5.22	SIS18 extraction kicker. . . . .	99
5.23	A possible triggering delay between extraction kicker magnets in the SIS18 two tanks. . . . .	101
5.24	Maximum triggering delay between extraction kicker magnets in the SIS18 two tanks. . . . .	101

## LIST OF FIGURES

---

5.25	The minimum triggering delay between extraction kicker magnets in two SIS18 tanks. . . . .	101
5.26	SIS100 injection kicker. . . . .	103
5.27	Schematic of the test setup. . . . .	104
5.28	Front view of the test setup. . . . .	105
5.29	Schematic of the final setup. . . . .	106
5.30	Flowchart of the firmware of the B2B source SCU for the test setup. .	108
5.31	Flowchart of the firmware of the B2B target SCU for the test setup. .	108
5.32	Flowchart of the firmware of the Trigger SCU for the test setup. . . .	109
B.1	Timing frames transfer for the B2B transfer . . . . .	156
F.1	The configuration of the packETH. . . . .	167



# List of Tables

5.1	Acceptable range of the parameters accompanying with the frequency adjustment of the phase shift method for the SIS18 $H^+$ and $U^{28+}$ beams	64
5.2	Acceptable range of the parameters accompanying with the frequency adjustment of the frequency beating method for the SIS18 $H^+$ and $U^{28+}$ beams . . . . .	64
5.3	Maximum orbit length displacement of three cases . . . . .	69
5.4	Maximum relative momentum shift of three cases . . . . .	70
5.5	Minimum bucket area factor of three cases . . . . .	72
5.6	Maximum adiabaticity of three cases . . . . .	72
5.7	Parameters accompanying with a 7 ms sinusoidal modulation for the SIS18 $H^+$ beam . . . . .	74
5.8	Parameters accompanying with a 50 ms sinusoidal modulation for the SIS18 $H^+$ beam . . . . .	74
5.9	Uncertainty of the phase alignment of all FAIR B2B use cases . . . .	79
5.10	Traffic produced by the XenaBay ports of the test setup . . . . .	87
5.11	The maximum frame transfer latency of the B2B Broadcast frames for different number of WR switch layers . . . . .	90
5.12	The 45 days test result of the WR network for the B2B transfer . . .	90
5.13	The tolerable number of WR switch layers for the B2B related traffic	91
5.14	Calculated parameters related to the simultaneous trigger of the SIS18 extraction kicker magnets in a common tank . . . . .	100
5.15	The triggering delay for the extraction kicker magnets in the two SIS18 tanks . . . . .	102
5.16	Calculated parameters related to the simultaneous trigger of the SIS100 injection kicker magnets . . . . .	103
5.17	The running time of the tasks of the B2B source SCU firmware . . .	110
6.1	List of the FAIR B2B transfer use cases . . . . .	113
6.2	Parameters related to the B2B transfer when the circumference ratio is an integer and the large accelerator is the target . . . . .	114
6.3	Parameters related to the B2B transfer when the circumference ratio is an integer and the small accelerator is the target . . . . .	115
6.4	Parameters related to the $U^{28+}$ B2B transfer from the SIS18 to the SIS100 with the frequency beating method . . . . .	116
6.5	Parameters related to the $H^+$ B2B transfer from the SIS18 to the SIS100 with the frequency beating method . . . . .	116
6.6	Parameters related to the B2B transfer when the circumference ratio is close to an integer and the large accelerator is the target . . . . .	118

## LIST OF TABLES

---

6.7	Parameters related to the B2B transfer when the circumference ratio is close to an integer and the small accelerator is the target . . . . .	118
6.8	Parameters related to the h=4 B2B transfer from the SIS18 to the ESR with the frequency beating method . . . . .	119
6.9	Parameters related to the h=1 B2B transfer from the SIS18 to the ESR with the frequency beating method . . . . .	120
6.10	Parameters related to the B2B transfer from the ESR to the CRYRING with the frequency beating method . . . . .	120
6.11	Parameters related to the B2B transfer when the circumference ratio is far away from an integer and the large accelerator is the target . .	121
6.12	Parameters related to the B2B transfer when the circumference ratio is far away from an integer and the small accelerator is the target . .	122
6.13	Parameters related to the $H^+$ B2B transfer from the SIS100 to the CR with the frequency beating method . . . . .	123
6.14	Parameters related to the RIB B2B transfer from the SIS100 to the CR with the frequency beating method . . . . .	124
6.15	Parameters related to the B2B transfer from the CR to the HESR with the frequency beating method . . . . .	125
6.16	Parameters related to an applied case of the B2B transfer from the SIS18 to the ESR via the FRS with the frequency beating method . .	125
6.17	Summary of the formulas related to the B2B transfer when the large accelerator is the target . . . . .	127
6.18	Summary of the formulas related to the B2B transfer when the small accelerator is the target and the revolution period is longer than the period of the synchronization frequency of the target accelerator . . .	128
6.19	Summary of the formulas related to the B2B transfer when the small accelerator is the target and the revolution period is shorter than the period of the synchronization frequency of the target accelerator . . .	129
A.1	B2B timing frames . . . . .	154
C.1	Parameters related to the B2B transfer from the SIS18 to the SIS100	157
C.2	Parameters related to the B2B transfer from the SIS18 to the ESR . .	158
C.3	Parameters related to the B2B transfer from the SIS18 to the ESR via the FRS . . . . .	159
C.4	Parameters related to the B2B transfer from the ESR to the CRYRING	160
C.5	Parameters related to the B2B transfer from the CR to the HESR . .	161
C.6	Parameters related to the B2B transfer from the SIS100 to the CR . .	162
D.1	Parameters for the B2B transfer provided by SM . . . . .	164
E.1	Parameters of kicker magnets . . . . .	165



# Publications

- 2015 J. Bai, T. Ferrand, D. Beck, R. Bär, O. Kester, D. Ondreka, C. Prados, and W. Terpstra. Bunch to Bucket Transfer System for FAIR. In *Proc. of ICALEPCS*, Melbourne, Australia, 2015
- T. Ferrand and J. Bai. System Design for a deterministic Bunch-to-Bucket Transfer. In *Proc. of IPAC*, Richmond, VA, USA, 2015
- 2014 J. Bai, D. Beck, R. Bär, D. Ondreka, T. Ferrand, M. Kreider, C. Prados, S. Rauch, W. Terpstra, and M. Zweig. First Idea on Bunch to Bucket Transfer for FAIR. In *Proc. of PCaPAC*, Karlsruhe, Germany, 2014
- M. Kreider, J. Bai, R. Bär, D. Beck, A. Hahn, C. Prados, S. Rauch, W. W. Terpstra, and M. Zweig. Launching the FAIR Timing System with CRYRING. In *Proc. of PCaPAC*, Karlsruhe, Germany, 2014
- T. Ferrand and J. Bai. System Simulation of Bunch-to-Bucket Transfer Between Synchrotrons. *GSI Scientific Report*, 2014
- 2013 J. Bai, L. Zeng, B. Wang, P. Li, F. Li, T. Xu, and Z. Li. Modified Read-out System of the Beam Phase Measurement System for CSNS. *Chinese physics C*, 37(10):107004, 2013
- D. Beck, J. Adamczewski-Musch, J. Bai, R. Bär, J. Frhauf, J. Hoffmann, M. Kreider, N. Kurz, C. Prados, S. Rauch, S. Voltz, and M. Zweig. Paving the Way for the General Machine Timing System. *GSI Scientific Report*, 2013
- M. Kreider, J. Bai, D. Beck, C. Prados, W. Terpstra, S. Rauch, and M. Zweig. Receiver Nodes of the General Machine Timing System for FAIR and GSI. *GSI Internal Document*, 2014
- 2012 J. Bai, S. Xiao, T. Xu, and L. Zeng. The Development of Timing Control System for RFQ. In *Proc. of LINAC*, Tel Aviv, Israel, 2012

# Jiaoni Bai

---

## Curriculum Vitae

*"I am a slow walker, but I never stop walking." - Jiaoni Bai*

---

### Education

- 2013–Now **PhD of physics**, *Goethe-Universität, Frankfurt am Main, Germany.*
- 2010–2013 **Master of Engineering Study in Computer Technology**, *Institute of High Energy Physics, Chinese Academy of Sciences, Peking, China, GPA – 8.0.*
- 2006–2010 **Bachelor of Engineering Study in Medical Informatics Engineering**, *Southern Medical University, Guangzhou, China, GPA – 9.0.*

---

### PhD Dissertation

- Title *Development of the timing system for the Bunch-to-Bucket transfer between the FAIR accelerators*
- Professor Prof. Dr. Oliver Kester
- Supervisors Dr. Dietrich Beck and Dr. David Ondreka
- Description
  - Development of the Bunch-to-Bucket transfer system
  - C-programming of the soft CPU LatticeMico32
  - VHDL programming of Altera FPGAs
  - Measurement of the White Rabbit network performance

---

### Master Thesis

- Title *The development of EPICS driver for customized VME hardware*
- Supervisor Taoguang Xu
- Description
  - Development of the software interface between EPICS and VME hardware
  - Development of the operator controlling and monitoring interfaces by MEDM hardware
  - VxWorks program for Motorola VME board MVME5100

---

### Bachelor Thesis

- Title *The CCD performance test and analysis*

Römergasse 10 – 64291 Darmstadt, Germany  
☎ (49) 017682537175 • 📞 (49) 6159 71 3126  
✉ baijiaoni1314@gmail.com

- Description
- Investigation of the influence factors for CCD
  - Test how these factors influence CCD

---

## Awards

- 2012 Won “Scholarship of the head of the Institute of High Energy Physics, CAS” for master thesis
- 2007 Won second prize of “Mathematical Contest in Modeling in Southern Medical University”

---

## Key skills

- Intermediate Network engineering, Bash shell script and Visual Basic programming
- Advanced VHDL program for Altera FPGAs, C, accelerator technology, accelerator physics, VxWorks programming and EPICS

---

## Computer literacy

- Basic applications Windows, Linux (Ubuntu/Debian), Microsoft Office and LaTeX
- Engineering applications Altera Quartus and Matlab
- Art design application Photoshop and Corel VideoStudio
- Web design Dreamweaver

---

## Languages

- Mandarin Chinese Mother tongue
- English Good written and spoken
- German Goethe-Zertifikat B2